SCIENCE CHINA
Chemistry

• ARTICLES •
• SPECIAL ISSUE • In Honor of the 80th Birthday of Professor WANG Fosong

May 2012 Vol.55 No.5: 772–778
doi: 10.1007/s11426-012-4528-7

# Preparation and self-assembly of amphiphilic polymer with aggregation-induced emission characteristics

QIN AnJun[1*], ZHANG Ya[2], HAN Ning[3], MEI Ju[1], SUN JingZhi[1], FAN WeiMin[3] & TANG Ben Zhong[1,4*]

[1]*MOE Key Laboratory of Macromolecular Synthesis and Functionalization; Department of Polymer Science and Engineering, Zhejiang University, Hangzhou 310027, China*
[2]*Department of Chemistry, Zhejiang University, Hangzhou 310027, China*
[3]*College of Medicine, Zhejiang University, Hangzhou 310027, China*
[4]*Department of Chemistry, Institute of Molecular Functional Materials, State Key Laboratory of Molecular Neuroscience, The Hong Kong University of Science & Technology, Clear Water Bay, Kowloon, Hong Kong, China*

Received November 30, 2011; accepted December 22, 2011; published online March 12, 2012

An amphiphilic polymer bearing tetraphenylethene (TPE) moiety was synthesized by convenient reactions. The polymer exhibits unique aggregation-induced emission (AIE) characteristics and can self-assemble to size-tunable particles in DMF/water mixtures. The polymer nanoparticles can be used for cell imaging, which provides a potential stable fluorescent tool to monitor the distribution of drugs and bioconjugates in living cells.

**amphiphilic polymer, aggregation-induced emission, tetraphenylethene, self-assembly, cell imaging**

## 1 Introduction

It has been a textbook knowledge that conventional luminescent materials are highly emissive in their dilute solutions with fluorescent quantum yields reaching unity. However, their emission could be partially or completely quenched by the aggregation [1]. This photophysical process is well-known as aggregation-caused quenching (ACQ), which has greatly limited the technological application scopes of these luminophores, because most of them are commonly used in the solid state (e.g., as thin films) in real-world applications. Various chemical, physical and engineering approaches have been taken to interfere with luminophore aggregation, but the attempts have met with only limited success [2–4].

Exactly opposite to the notorious ACQ effect, our group has discovered an unusual phenomenon: propeller-shaped molecules are virtually non-luminescent when they are dissolved in their good solvents as isolated species but become highly emissive when they are aggregated into nanoparticles in their poor solvents or fabricated into thin films in the solid state [5]. We thus coined the term of aggregation-induced emission (AIE) for this extraordinary phenomenon, because these molecules were induced to emit by aggregate formation.

Since then, scientists have been actively involved in the synthesis of new AIE systems and exploration of their potential applications. A large number of AIE-active luminogens and polymers have been developed for diverse applications, for example, in the areas of stimuli-responsive nanomaterials, and organic light-emitting diodes [6, 7]. Particularly, the AIE luminogens have shown their unique properties in the detection of bioconjugates, such as DNA, saccharides, and protein, based on their mechanism of restriction of intramolecular rotation [8–13] and can be regarded as the organic version of quantum dots.

*Corresponding author (email: qinaj@zju.edu.cn; tangbenz@ust.hk)

However, the AIE luminogens have been rarely incorporated in amphiphilic systems, which could self-assemble to form nanoparticles [14]. It will be extremely attractive to prepare such nanoparticles from amphiphilic polymers that exhibit AIE feature, which are promising to deliver drugs and DNA, and allow us to monitor cellular distribution of the drugs at the same time [15]. The essence of the present work is to synthesize amphiphilic polymers bearing AIE luminogen as their pendant, to prepare size tunable fluorescent nanoparticles, and to investigate the photophysical properties of both the polymers and nanoparticles.

## 2 Experimental

### 2.1 General information

The starting materials used for the synthesis of intermediates **1** and **2** as well as the P**I** were purchased from Alfa, Acros and Aladdin. They were used without further purification. All the solvents used were freshly dried. FT-IR analysis was conducted on a BURKER VECTOR 22 FT-IR spectrometer. $^1$H NMR spectra were measured on a Bruker DMX 300 NMR spectrometer in $CDCl_3$ using tetramethylsilane (TMS, $\delta = 0$) as internal reference. Thermogravimetric (TGA) analyses and differential scanning calorimetry (DSC) studies were conducted on Perkin Elmer Pyris 6 under nitrogen at a heating rate of 10 °C/min. Photoluminescence (PL) spectra were measured on a Perkin Elmer LS 55 Spectrofluorometer. $M_w$, $M_n$ and $M_w/M_n$ or PDI values of the polymer were estimated by a Waters 150 C GPC system, using *N*,*N*-dimethylformamide (DMF) as the eluent at a flow rate of 1.0 mL/min and a set of monodisperse polystyrenes as calibration standards. The dynamic light scattering (DLS) analysis was conducted on a Brookhaven90 plus spectrometer. SEM study was conducted on JSM-5510.

### 2.2 Synthesis of amphiphilic polymer PII

To a 250 mL two-necked, round-bottom flask were added poly(*N*-methyldietheneamine sebacate) (P**I**) (3.574 g, 9.03 mmol) and cholesterol derivative (**1**) (4.97 g, 9.04 mmol). Then the flask was vacuum-evacuated and refilled with dry nitrogen three times. Freshly distilled toluene (50 mL) was injected and the mixture was refluxed under nitrogen for two days. Afterwards, the solution of 1-[(4-bromomethyl)-phenyl)]-1,2,2-triphenylethene (**2**) (1.203 g, 2.83 mmol) in dry toluene was injected under nitrogen. The solution continued to reflux for an additional one day. Then the mixture was cooled down and added dropwise into 500 mL $Et_2O$ under vigorous stirring. The precipitate was allowed to stand overnight, collected by filtration, washed three times by $Et_2O$, and dried under vacuum at 40 °C to a constant weight. Brown viscous product of P**II** was obtained in a yield of 31.6%. $M_w$: 18800, PDI (GPC, polystyrene calibration): 1.58. IR (KBr) $\nu$ = 1736, 1463, 1243, 1116, 735, 701. $^1$H NMR (300 MHz, $CDCl_3$, δ): 7.07, 7.00, 5.35, 4.60, 4.44, 4.12, 3.45, 2.79, 2.35, 1.83, 1.59, 1.29, 1.11, 0.99, 0.86, 0.66.

### 2.3 MTT assay

Human breast cancer BCap37 cells were purchased from ATCC. Drug resistant breast cancer cell line-Bats72 was established from BCap37 cell line via a two-stage screening strategy using paclitaxel as a selective drug. Both BCap37 and Bats72 cells were cultured in RPMI1640 (Gibco, USA) supplemented with 10% fatal bovine serum (FBS) (Sijiqing Biological Engineering Materials Co., Ltd.).

BCap37 and Bats72 cells were seeded onto 96-well plates at a density of $1.2 \times 10^4$ cells/well, cultured in 100 μL growth medium, and incubated for 24 h (5% $CO_2$, 37 °C) to reach 70%–80% confluency before nanoparticle addition. The nanoparticles, which were prepared in DMF/water mixture with 99% water fraction, were dispersed in cell culture medium at two different concentrations (15 and 30 mg/L). When the desired cell confluency was reached, 100 μL of the pre-prepared nanoparticle solution was added into each well following the removal of the spent growth medium. Each condition was tested in 10 replicates. The plates were then incubated for 48 h (5% $CO_2$, 37 °C).

Next, the nanoparticle solution was removed from each well and replaced with the mixture of 15 μL of 3-(4,5-dimethylthiazol-2-yl)-2,5-diphenyltetrazolium bromide (MTT) solution and 100 μL of fresh cell culture medium. The samples were cultivated in an incubator for a further 3 h (5% $CO_2$, 37 °C). After removing the culture medium and excess MTT solution from each well, 200 μL DMSO was added into each well to dissolve the internalized purple formazan crystals. An aliquot of 100 μL was transferred from each well to a new 96-well plate. The new plates were analyzed at 570 nm using a microplate reader (BIO-RAD, Model 680, USA). The absorbance readings of the formazan crystals were recorded as $A_{570}$. The results were expressed as cell viability = $A_{570}$ (sample)/$A_{570}$(control) × 100%.

### 2.4 Cell imaging

Polylysine pre-treated cover glass was placed in each well of a 6-well plate. BCap37 cells were seeded onto the 6-well plate at a density of $2 \times 10^5$ cells/well, cultivated in 2 mL of growth medium, and incubated overnight at 5% $CO_2$, 37 °C. The next day, the spent growth medium was replaced with 2 mL of the pre-prepared 15 mg/L nanoparticle solution. Afterwards, the cells were incubated with the fluorescent nanoparticles for 1 h, and then washed with PBS, stained with DAPI, and fixed with 4 wt% paraformaldehyde in PBS. The cell-attached cover glasses were transferred from each well to glass slides, and imaged at 10 and 20-fold magnifications using confocal microscopy (Carl Zeiss, USA). BCap37 cells cultivated without the fluorescent nanoparticles were tested as controls. Each condition was performed in triplicates.

## 3 Results and discussion

### 3.1 Synthesis of amphiphilic polymer PII

Among the AIE luminogens, tetraphenylethene (TPE) moiety has drawn much attention because of its facile preparation, ready functionalization, good photostability, and high PL efficiency [16–23]. To demonstrate our design is rational, we used TPE derivative as the AIE pendant in the amphiphilic polymer. The cholesterol derivative **1** and poly(*N*-methyldietheneamine sebacate) (P**I**) were synthesized according to the published procedures [15]. TPE derivative **2** was synthesized according to the synthetic routes shown in Scheme 1. Lithiation of diphenylmethane (**3**) followed by reaction with 4-methylbenzophenone (**4**) generated **5**, which underwent dehydration in the presence of *p*-toluenesulfonic acid to form 1-(4-methylphenyl)-1,2,3-triphenylethene (**6**). Bromination of **6** with *N*-bromosuccinimide in refluxed carbon tetrachloride readily furnished the intermediate of 1-[(4-bromomethyl)phenyl)]-1,2,2-triphenylethene (**2**). The amphiphilic polymer P**II** was synthesized by the quaterization reaction (Scheme 2). Chelosterol derivative **1** was first added to the toluene solution of P**I** and the mixture was allowed to reflux for 48 h. Then, TPE derivative **2** was added and the solution was refluxed for an additional 24 h. The P**II** with $M_w$ of 18800 was obtained in 31.6% yield. The polymer is soluble in DMF but partially soluble in chloroform, and is thermally stable, with 5% loss of its weight at a temperature of 222 °C.

### 3.2 Structural characterization

Although the polymer is partially soluble in chloroform, we used $CDCl_3$ as a solvent to measure the $^1$H NMR spectra because they still possess high resolution. Figure 1 shows the $^1$H NMR spectra of P**II** as well as its intermediates of P**I** and **1**. The methylene protons adjacent to the ester groups in **1**, the ethenyl protons in P**I**, and the aromatic protons in **2** resonate at $\delta$ 4.14, 5.39, and 7.00–7.07, respectively, which are all present in P**II** (labeled as a, b, and Ar respectively). Furthermore, the methylene protons adjacent to the bromo groups in **1** and **2** all shifted to up-field after reaction, manifesting that the hydrophobic cholesterol and TPE moieties have been successfully grafted to the P**I** after quaterization reaction.

Since the peaks of Ar, b and a in the spectrum of P**II** are free from overlapping by other resonances, we used them to calculate the grafting ratio of cholesterol and TPE moieties, which are deduced as 24.0% and 16.2%, respectively. The appearance of resonance of carbon at δ 162 and 133–126 in $^{13}$C NMR spectrum of P**II** further substantiates the conclusion drawn from the $^1$H NMR spectra (Figure 2).

### 3.3 Aggregation-induced emission

TPE is characterized by its AIE attribute: it is virtually nonluminescent when molecularly dissolved in its good solvents but emits intensely when aggregated in its poor solvent or fabricated into thin solid film. Dose the TPE-containing P**II** possess the similar feature? To answer

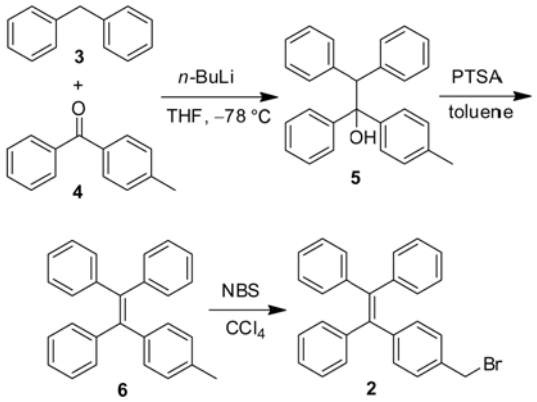


**Scheme 1** Synthetic routes to TPE derivative **2**. PTSA = *p*-toluenesulfonic acid, NBS = *N*-bromosuccinimide.

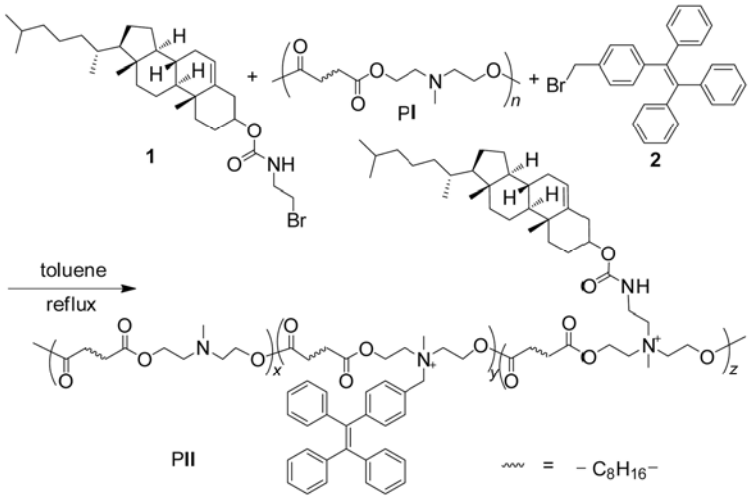


**Scheme 2** Synthesis of TPE and cholesterol containing amphiphilic polymer P**II**.

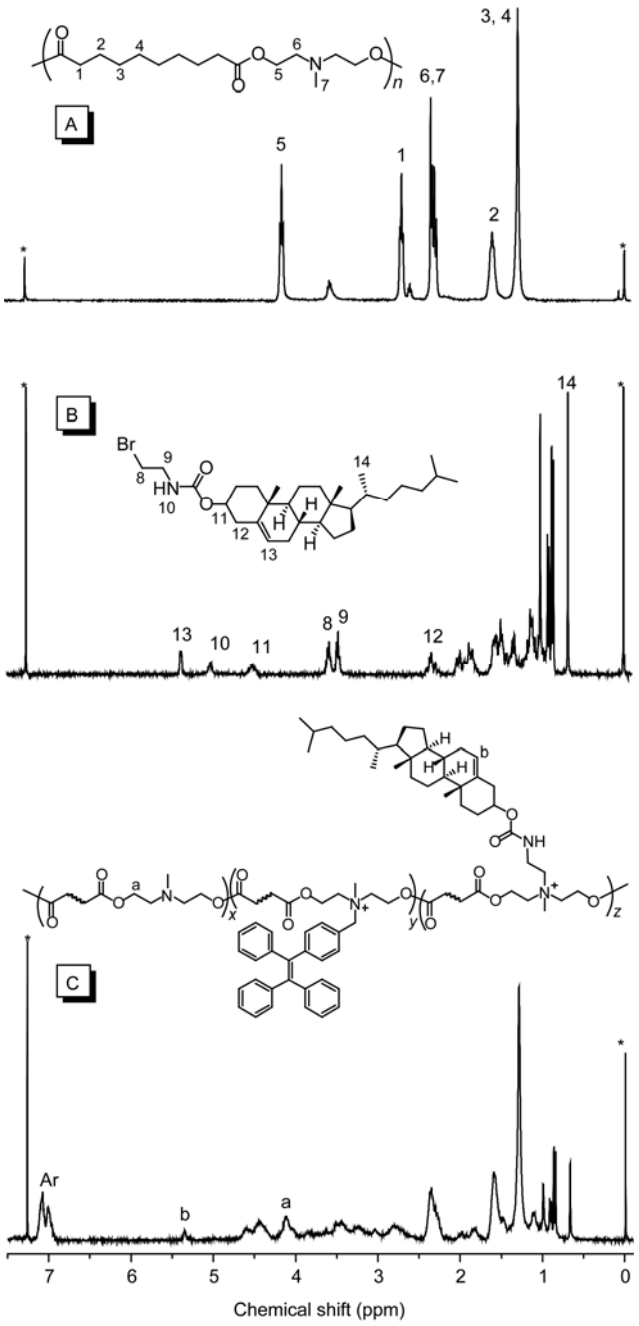


**Figure 1** $^{1}$H NMR spectra of (A) P**I**, (B) **1**, and (C) P**II** in $CDCl_3$ at room temperature. The solvent peaks are marked with asterisks.

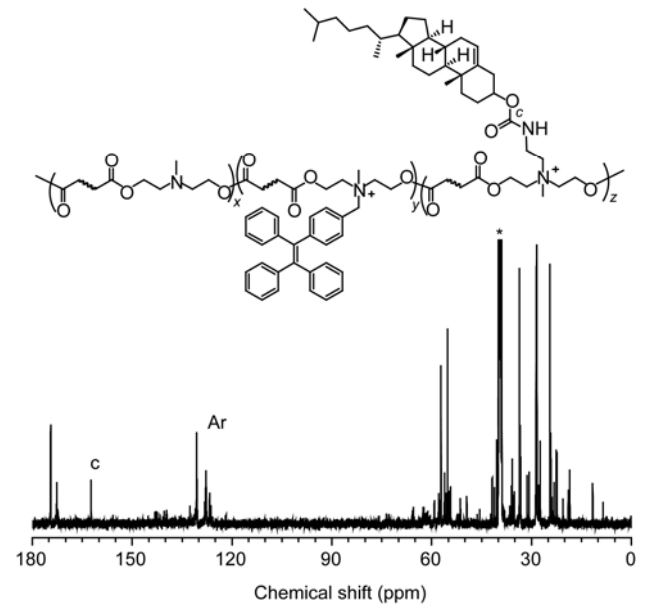


**Figure 2** $^{13}$C NMR spectrum of P**II** in DMSO-$d_6$ at room temperature. The solvent peaks are marked with asterisks.

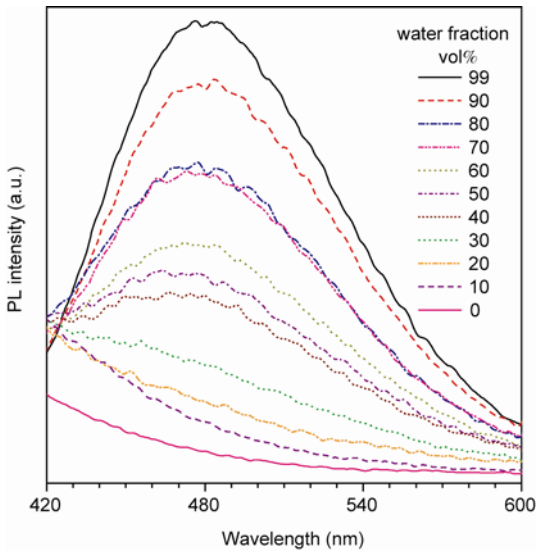


**Figure 3** PL spectra of P**II** in DMF and DMF/water mixtures. Polymer concentration: 3.252 mg/L; excitation wavelength: 340 nm.

this question, we investigated the PL behaviors of P**II** in the solution and aggregate states. Since P**II** is soluble in DMF, we then dissolved the polymer in DMF for AIE characterization. The aggregates were prepared by adding water into the DMF solution under vigorous stirring. The absorption spectrum of P**II** in DMF exhibits a maximum peak at 340 nm that corresponds to the electronic absorption of the TPE moiety.

When excited at 340 nm, the DMF solution is non-emissive, manifesting that P**II** is a weak emitter when it is molecularly dissolved. With addition of water into the solution, an intense PL peak centered at ~480 nm was recorded (Figure 3). Furthermore, the emission was continuously intensified with gradual addition water. The highest emission was obtained in DMF/water mixtures with 99% water fraction. These results indicate that P**II** is AIE-active.

The *N*-methyldietheneamine sebacate units in the backbone, the cholesterol and TPE moieties are hydrophobic, but the quaternary ammonium salt segments are hydrophilic. These amphiphilic characteristics make P**II** form aggregates upon addition of water, in which the hydrophobic moieties come together to form the inner core and the phenyl rotation of TPE moieties should be remarkably restricted in the crowed environment and its emission is turned on accordingly.

### 3.4 Aggregate morphology

The morphology of the aggregates was investigated by scanning electron microscopy (SEM). The samples were prepared by adding water into the DMF solution of P**II** and the aqueous mixtures were stood for 3 h to allow the polymer to be well self-assembled. Then, the aqueous mixture was dropped on a silica grid and the solvents were allowed to evaporate. As shown in Figure 4(a), P**II** aggregates into particles in the aqueous mixtures. More interestingly, the sizes of the aggregates are tunable and the diameter of the aggregates ranges from ~2 μm to 50 nm. Furthermore, the particle sizes decreased and their surface turned to be smoother with increasing the water fraction in the DMF/water mixtures. When the polymer is dissolved in its good solvent, the driving force for it to self-assemble is weak. Thus, the polymer chain tends to assemble loosely and entangle more randomly. Whereas, in the DMF/water mixtures with higher water fraction, the environment becomes more hydrophilic, the polymer orientates itself in order to remove the hydrophobic part from the hydrophilic environment, which results in tighter aggregates. Thanks to the AIE feature of the polymer, its aggregates are emissive. Although the resolution is not high, bluish-green light of the particles was observed under the fluorescent microscopy (Figure 4(b)).

To verify the size trends of the particles, we performed the dynamic light scattering (DLS) measurement using the aggregates prepared from DMF/water mixtures with water fraction of 0, 40%, 90%, and 99%. The particle sizes are obtained as 1718, 459, 51, and 59 nm, respectively, further substantiating the observation from SEM. It is noteworthy that the particle sizes remain almost unchanged within the experimental errors in the DMF/water mixture with water fraction larger than 90%, suggesting that the self-assembly process was performed by several or even one polymer chain.

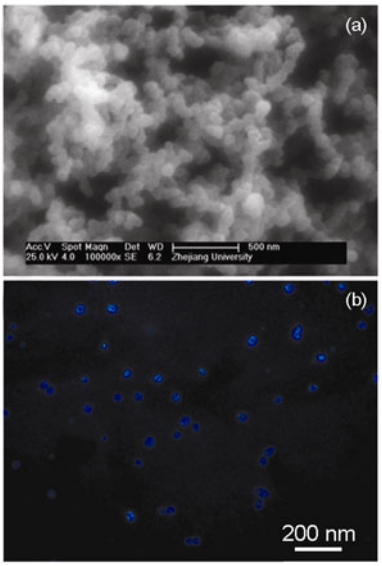


**Figure 4** (a) SEM image of P**II** particles, prepared in the DMF/water mixture with 99% water fraction. (b) Fluorescent particles observed under a fluorescent microscope. The sample was obtained in DMF/water mixture with 90% water fraction.

### 3.5 Cell imaging

With the AIE-active amphiphilic polymer in hand, we investigated its potential application for bio-imaging. We first evaluated the cytotoxicity of its nanoparticles, which are to be used for cell imaging and prepared in the DMF/water mixtures with 99% water fraction, via classic MTT assay [24]. As shown in Figure 5, the nanoparticles of P**II** displayed different cytotoxicity to Human breast cancer BCap37 cells and multidrug-resistant Bats72 cells. The former did not show significant decrease in cell viability when treated with either 15 or 30 mg/L nanoparticle solution [statistical significance ($p$) > 0.05], whereas the addi-

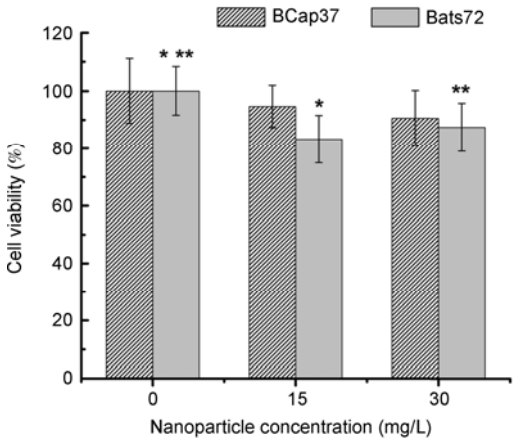


**Figure 5** Viability of BCap37 and Bats72 cells after being incubated with the nanoparticles of P**II**. Samples with the same number of asterisks are significantly different ($p < 0.05$).

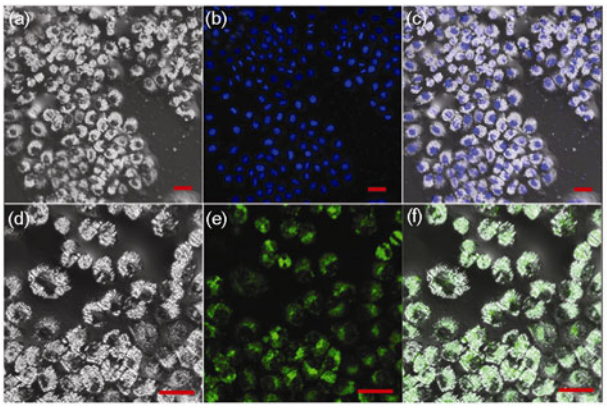


**Figure 6** Cellular distribution of the nanoparticles of P**II** in BCap37. (a–c) control: BCap37 cells. Nuclei are stained with 4',6-diamidino-2-phenylindole, and the cytoplasm is shown as light gray dots. (d–f) BCap37 cells incubated with the nanoparticles (concentration: 15 mg/L). The nanoparticle is shown as green fluorescence in the cytosol. Scale bars: 20 μm.

tion of nanoparticle solutions (i.e., 15 and 30 mg/L) led to a remarkable reduction of Bats72 cell viability ($p < 0.05$). The slight cytotoxicity of the nanoparticles of P**II** could probably be ascribed to the cationic quaternary ammonium salt, which was located on the surface of the aggregates.

Since the nanoparticles are less cytotoxic to BCap37, we used these cells for imaging. Cellular uptake and distribution of the nanoparticles was studied using confocal microscopy. Figure 6(a–c) displays the morphology of control BCap37 cells without the treatment of nanoparticles.

The cytoplasm is shown as light gray dots in Figure 6(a), and nuclei are stained blue with 4',6-diamidino-2-phenyl-indole (DAPI) in Figure 6(b). Figure 6(c) is the composite image of Figure 6(a) and 6(b). As shown in Figure 6(d–f), no significant morphological change of BCap37 cells was observed after the cellular delivery and uptake of the nanoparticles. The green emission particles were found mostly accumulated in the cytosol rather than the nucleus.

## 4 Conclusions

In summary, the amphiphilic polymer P**II** with $M_w$ of 18800 was synthesized by incorporation of hydrophobic cholesterol and TPE moieties via facile quaterization reactions. The obtained P**II** was thermally stable, soluble in DMF, and can self-assemble to particles in the DMF/water mixture with the hydrophobic moieties in the inner core, which results in high emission due to the AIE feature of TPE. Furthermore, the particle sizes can be tuned with water fraction in the aqueous solution and the surface became smoother in higher water fractions. The emissive particles are less cytotoxic to BCap37 and can be used for cellular imaging. The results demonstrate that the particles are accumulated in the cytosol rather than the nucleus. Thus, the high internalization of the nanoparticles in BCap37 cells displayed their great potentials in both bio-imaging and controlled drug delivery.

*This work was partially supported by the National Natural Science Foundation of China (20974028, 20974098, and 21174120); the National Basic Research Program of China (2009CB623605), and the Research Grants Council of Hong Kong (603509, HKUST2/CRF/10, 604711, and N_HKUST620/11). B.Z.T. thanks the support from the Cao Guangbiao Foundation of Zhejiang University.*

1 Birks JB. *Photophysics of Aromatic Molecules*. Wiley, London, 1970
2 Wang J, Zhao Y, Dou YC, Sun H, Xu P, Ye K, Zhang J, Jing S, Li F, Wang Y. Alkyl and dendron substituted quinacridones: Synthesis, structures, and luminescent properties. *J Phys Chem B*, 2007, 111: 5082–5089
3 Hecht S, Frechet JMJ. Dendritic encapsulation of function: Applying nature's site isolation principle from biomimetics to materials science. *Angew Chem Int Ed*, 2001, 40: 74–91
4 Chen L, Xu S, McBranch D, Whitten D. Tuning the properties of conjugated polyelectrolytes through surfactant complexation. *J Am Chem Soc*, 2000, 122: 9302–9303
5 Luo JD, Xie ZL, Lam JWY, Cheng L, Chen HY, Qiu CF, Kwok HS, Zhan XW, Liu YQ, Zhu DB, Tang BZ. Aggregation-induced emission of 1-methyl-1,2,3,4,5-pentaphenylsilole. *Chem Commun*, 2001, 1740–1741
6 Hong YN, Lam JWY, Tang BZ. Aggregation-induced emission. *Chem Soc Rev*, 2011, 40: 5361–5388
7 Hong YN, Lam JWY, Tang BZ. Aggregation-induced emission: Phenomenon, mechanism and application. *Chem Commun*, 2009, 4332–4353
8 Chen JW, Law CCW, Lam JWY, Dong YP, Lo SMF, Williams ID, Zhu DB, Tang BZ. Synthesis, light emission, nanoaggregation, and restricted intramolecular rotation of 1,1-substituted 2,3,4,5-tetraphenylsiloles. *Chem Mater*, 2003, 15: 1535–1546
9 Zhang S, Qin AJ, Sun JZ, Tang BZ. Progress in mechanism study of aggregation-induced emission (in Chinese). *Prog Chem*, 2011, 23: 623–636
10 Li Z, Dong YQ, Mi BX, Tang YH, Haussler M, Tong H, Dong YP, Lam JWY, Ren Y, Sung HHY, Wong KS, Gao P, Williams ID, Kwok HS, Tang BZ. Structural control of the photoluminescence of silole regioisomers and their utility as sensitive regiodiscriminating chemosensors and efficient electroluminescent materials. *J Phys Chem B*, 2005, 109: 10061–10069
11 Li Z, Dong YQ, Lam JWY, Sun JX, Qin AJ, Häußler M, Dong YP, Sung HHY, Williams ID, Kwok HS, Tang BZ. Functionalized siloles: Versatile synthesis, aggregation-induced emission, and sensory and device applications. *Adv Funct Mater*, 2009, 19: 905–917
12 Zeng Q, Li Z, Dong YQ, Di CA, Qin AJ, Hong YN, Ji L, Zhu ZC, Jim CKW, Yu G, Li QQ, Li ZA, Liu YQ, Qin JG, Tang BZ. Fluorescence enhancements of benzene-cored luminophors by restricted intramolecular rotations: AIE and AIEE effects. *Chem Commun*, 2007, 70–72
13 Qian LJ, Zhi JG, Tong B, Yang F, Zhao W, Dong YP. Organic compounds with aggregation-induced emission (in Chinese). *Prog Chem*, 2008, 20: 673–678
14 Tang HW, Xing CF, Liu LB, Yang Q, Wang S. Synthesis of amphiphilic polythiophene for cell imaging and monitoring the cellular distribution of a cisplatin anticancer drug. *Small*, 2011, 7: 1464–1470
15 Wang Y, Gao SJ, Ye WH, Yoon HS, Yang YY. Co-delivery of drugs and DNA from cationic core-shell nanoparticles self-assembled from a biodegradable copolymer. *Nature Mater*, 2006, 5: 791–796
16 Dong YQ, Lam JWY, Qin AJ, Liu JZ, Li Z, Tang BZ, Sun JX, Kwok SH. Aggregation-induced emissions of tetraphenylethene derivatives and their utilities as chemical vapor sensors and in organic light-emitting diodes. *Appl Phys Lett*, 2007, 91: 011111
17 Qin AJ, Lam JWY, Tang L, Jim CKW, Zhao H, Sun JZ, Tang BZ. Polytriazoles with aggregation-induced emission characteristics: Synthesis by click polymerization and application as explosive chemosensors. *Macromolecules*, 2009, 42: 1421–1424
18 Wang J, Mei J, Yuan WZ, Lu P, Qin AJ, Sun JZ, Ma YG, Tang BZ. Hyperbranched polytriazoles with high molecular compressibility: aggregation-induced emission and superamplified explosive detection. *J Mater Chem*, 2011, 21:4056–4059
19 Li HY, Chi ZG, Xu BJ, Zhang XQ, Li XF, Liu SW, Zhang Y, Xu JR. Aggregation-induced emission enhancement compounds containing triphenylamine-anthrylenevinylene and tetraphenylethene moieties. *J Mater Chem*, 2011, 21: 3760–3767
20 Chen Q, Zhang DQ, Zhang GX, Yang XY, Feng Y, Fan QH, Zhu DB. Multicolor tunable emission from organogels containing tetraphenylethene, perylenediimide, and spiropyran derivatives. *Adv Funct Mater* 2010, 20: 3244–3251
21 Wang M, Zhang GX, Zhang DQ, Zhu DB, Tang BZ. Fluorescent

bio/chemosensors based on silole and tetraphenylethene luminogens with aggregation-induced emission feature. *J Mater Chem*, 2010, 20: 1858–1867

22 Yuan WZ, Lu P, Chen SM, Lam JWY, Wang ZM, Liu Y, Kwok HS, Ma YG, Tang BZ. Changing the behavior of chromophores from aggregation-caused quenching to aggregation-induced emission: development of highly efficient light emitters in the solid state. *Adv Mater,* 2010, 22: 2159–2163

23 Zhao ZJ, Chen SM, Lam JWY, Lu P, Zhong YC, Wong KS, Kwok HS, Tang BZ. Creation of highly efficient solid emitter by decorating pyrene core with AIE-active tetraphenylethene peripheries. *Chem Commun*, 2010, 2221–2223

24 Denizot F, Lang R. Rapid colorimetric assay for cell growth and survival: Modifications to the tetrazolium dye procedure giving improved sensitivity and reliability. *J Immunol Methods*, 1986, 89: 271–277